Cell

A Two-Hit Trigger for siRNA Biogenesis in Plants

Michael J. Axtell,[1,2,3] Calvin Jan,[1,2] Ramya Rajagopalan,[1,2] and David P. Bartel[1,2,*]
[1] Howard Hughes Medical Institute, Department of Biology, Massachusetts Institute of Technology, Cambridge, MA, USA
[2] Whitehead Institute for Biomedical Research, 9 Cambridge Center, Cambridge, MA 02142, USA
[3] Present address: Department of Biology, The Huck Institutes of the Life Sciences, Pennsylvania State University, 101 LSB., University Park, PA 16802, USA.
*Contact: dbartel@wi.mit.edu
DOI 10.1016/j.cell.2006.09.032

SUMMARY

In *Arabidopsis*, microRNA-directed cleavage can define one end of RNAs that then generate phased siRNAs. However, most miRNA-targeted RNAs do not spawn siRNAs, suggesting the existence of additional determinants within those that do. We find that in moss, phased siRNAs arise from regions flanked by dual miR390 cleavage sites. *AtTAS3*, an siRNA locus important for development and conserved among higher plants, also has dual miR390 complementary sites. Both sites bind miR390 in vitro and are functionally required in *Arabidopsis*, but cleavage is undetectable at the 5′ site—demonstrating that noncleavable sites can be functional in plants. Phased siRNAs also emanate from the bounded regions of every *Arabidopsis* gene with two known microRNA/siRNA complementary sites, but only rarely from genes with single sites. Therefore, two "hits,"—often, but not always, two cleavage events—constitute a conserved trigger for siRNA biogenesis, a finding with implications for recognition and silencing of aberrant RNA.

INTRODUCTION

MicroRNAs and endogenous siRNAs modulate the transcriptomes of both animals and plants (Bartel, 2004; Zamore and Haley, 2005). MicroRNAs are ~21-nt RNAs that are processed from primary transcripts with characteristic stem-loop secondary structures. siRNAs are processed from long double-stranded RNA (dsRNA) formed by convergent transcription, RNA-dependent RNA polymerization, or extended hairpin structures. Both miRNAs and siRNAs are incorporated into silencing complexes where they pair to target transcripts and mediate association between the silencing complexes and targeted transcripts.

Most characterized interactions involving miRNAs or siRNAs result in the negative regulation of the target, either at the transcriptional level (heterochromatic siRNAs) or at the posttranscriptional level (siRNAs and miRNAs; Bartel, 2004). Plant miRNAs have extensive pairing to their targets (Rhoades et al., 2002), and as a result, posttranscriptional repression generally is caused by mRNA cleavage (Llave et al., 2002; Tang et al., 2003). An interesting exception to the tendency to mediate repression comes with the finding that miRNA-directed cleavage is needed for the production of *trans*-acting siRNAs (tasiRNAs; Allen et al., 2005; Yoshikawa et al., 2005), which differ from classical siRNAs in that they silence messages from loci that are unrelated to those from which the siRNAs derive (Peragine et al., 2004; Vazquez et al., 2004b). Each tasiRNA locus (known as a *TAS* gene) produces a non-protein-coding transcript, a portion of which is converted by the RNA-dependent RNA polymerase (RdRp) RDR6 into dsRNA that in turn is successively cleaved into mostly 21-nt siRNAs by DCL4, a Dicer-like enzyme (Peragine et al., 2004; Vazquez et al., 2004b; Allen et al., 2005; Gasciolli et al., 2005; Xie et al., 2005; Yoshikawa et al., 2005). All known *Arabidopsis TAS* (*AtTAS*) loci have miRNA complementary sites at which miRNA-directed cleavage appears to define one end of the dsRNA intermediate, thereby setting the register of phased tasiRNA production (Allen et al., 2005; Yoshikawa et al., 2005). miR173 directs cleavage upstream of the *AtTAS1a-c* and *AtTAS2* siRNAs, whereas miR390 directs cleavage downstream of the *AtTAS3* siRNAs. This role for miRNAs in setting a phasing register for tasiRNA biogenesis is important because siRNAs produced in most other registers would not have sufficient homology to direct cleavage of their mRNA targets. The coupling of miRNA-mediated cleavage to RdRp activity and siRNA production for the *AtTAS* loci raises the question of why such transitivity is very rare for the majority of non-*TAS* miRNA targets (Lu et al., 2005), which also undergo miRNA-directed cleavage. It seems likely that endogenous miRNA targets that enter the *TAS* pathway possess additional, as of yet unknown molecular features beyond a single miRNA complementary site.

In this study, we adapt high-throughput DNA sequencing to the discovery of endogenous small RNAs from the

moss *Physcomitrella patens* and *Arabidopsis*. Our data demonstrate that *P. patens* has four loci that give rise to phased siRNAs resembling tasiRNAs. These moss siRNAs are in phase with cleavage sites for miR390, the same miRNA important for tasiRNA phasing in flowering plants (Allen et al., 2005). We find that the four moss siRNA loci are each flanked by dual miR390 complementary sites that are both cleaved in vivo. *AtTAS3* also has a second, conserved miR390 complementary site that had not been originally recognized; as in *P. patens*, the region that generates phased siRNAs falls between the two miR390 complementary sites. The newly identified upstream miR390 complementary site of *AtTAS3* is not cleaved, even though it binds an miR390-associated silencing complex in vitro and is necessary for full *AtTAS3* function in vivo, which indicates that conserved miRNA complementary sites can function independently of target cleavage in plants. We also find that *Arabidopsis* genes with two or more small RNA complementary sites universally produce phased siRNAs from the regions that fall between the sites. Our results indicate that dual miRNA complementary sites are a trigger for siRNA biogenesis that has been conserved for the past 400 million years and provide potential insights into the recognition and silencing of aberrant RNAs.

RESULTS

Endogenous Small RNAs from Moss

Small RNA was prepared from three developmentally staged samples of the moss *P. patens* and sequenced using either the standard di-deoxy method (Lau et al., 2001) or a recently described pyrosequencing technology (Margulies et al., 2005) to yield a total of 561,102 small RNA reads, representing 214,996 unique sequences (see Table S1 in the Supplemental Data). To begin to categorize these sequences, we compared them to the 5.4 million traces available at the time of our analysis from the *P. patens* whole-genome shotgun (WGS) project. A total of 127,135 unique small RNA sequences, represented by 384,441 reads, had at least one perfect match to the WGS traces (Table S1). The remaining sequences that did not perfectly match any WGS trace were not analyzed further and were presumed to be sequences from genomic regions missed by the WGS project, sequencing errors, or unclassified contaminant sequences. Some of the genome-matched sequences were classified as miRNAs (M.J.A. and D.P.B., unpublished data). These accounted for 42% of the genome-matched reads, leaving 58% that did not appear to arise from loci with the characteristics of known miRNAs, suggesting that, similar to *Arabidopsis*, *P. patens* might express many endogenous siRNAs. Among these potential siRNAs, 18% (39,975 reads representing 19,974 sequences) matched more than 1,000 traces, which would correspond to more than 100 endogenous loci; these were designated as repetitive small RNAs (Table S1). Once a genome assembly is available, it will be interesting to evaluate whether repeat elements are more or less likely than other regions of the genome to give rise to moss small RNAs.

The Antiquity of tasiRNAs

The first characterized tasiRNA loci showed no sign of conservation beyond *Arabidopsis* (Peragine et al., 2004; Vazquez et al., 2004b). However, two related tasiRNAs from the *AtTAS3* locus, required for the proper timing of vegetative development and regulation of organ polarity (Adenot et al., 2006; Fahlgren et al., 2006; Garcia et al., 2006; Hunter et al., 2006), are conserved among diverse flowering plants (Allen et al., 2005; Williams et al., 2005). To explore the possibility that tasiRNAs might have emerged much earlier in plant evolution, we searched the nonrepetitive WGS moss traces for clustered small RNA hits in both sense and antisense orientation, wherein a significant fraction were phased in ~21-nt increments. Four candidate tasiRNA loci were found (*PpTAS1-4*), one of which was represented by 15,730 reads—4.1% of all of the nonrepetitive, genome-matched reads (Figure 1A). Indeed, a cDNA corresponding to this locus (*PpTAS1*) had previously been suspected of being a tasiRNA precursor based on the sequencing of three corresponding small RNAs (Arazi et al., 2005).

All known *Arabidopsis* tasiRNA loci have miRNA complementary sites that are thought to be important for setting the register of phased siRNA production (Allen et al., 2005; Yoshikawa et al., 2005). We found that all four moss *TAS* loci had complementary sites for miR390 positioned so as to set the phasing register of the dominant siRNA species (Figure 1). miR390 is conserved throughout land plants (Axtell and Bartel, 2005) and is the same miRNA that sets the phasing register for the *AtTAS3* siRNAs (Allen et al., 2005). *PpTAS2* had one siRNA in common with *PpTAS1* and another in common with *PpTAS3*, but otherwise the four *P. patens TAS* loci shared little sequence identity beyond their miR390 complementary sites (Figure S1). Moreover, no sequences resembling the *Arabidopsis* tasiRNAs were discerned in any of the four *PpTAS* loci, begging the question as to the evolutionary relationship between the *TAS* loci of moss and those of higher plants. Nonetheless, the presence of miR390 complementary sites in the *PpTAS* loci supported the idea that these four loci were indeed tasiRNA genes and suggested that miR390 has been setting the phasing register of tasiRNAs since the last common ancestor of moss and angiosperms.

Surprisingly, each of the *PpTAS* loci contained not one but two miR390 complementary sites, one upstream and another downstream of the siRNA-corresponding region (Figure 1). The phasing register of the siRNAs was consistent with cleavage at both complementary sites: 71.3% of the *PpTAS*-derived small RNAs began within one nucleotide of the residues predicted by cleavage at either the 5′ or 3′ site. We confirmed miR390-mediated cleavage at both sites of *PpTAS1* using 5′-RACE (Llave et al., 2002); 11 out of 17 sequenced cleavage products had 5′ residues corresponding precisely to those predicted by

cleavage at either the 5′ or 3′ miR390 complementary site (Figure 1A). These observations indicate that tasiRNA biogenesis from *PpTAS* loci is triggered by two miR390-directed cleavage events that together define the intervening cleavage product as a substrate for subsequent RdRp and Dicer activity.

Dual miR390 Complementary Sites Are a Conserved Feature of tasiRNA Precursors

Having found two miR390 complementary sites in each of the four moss *TAS* loci, we examined the *AtTAS3* locus to see if it might also have two sites. A second miR390 site was found, located upstream of the tasiRNA region (Figure 2A). Pyrosequencing of small RNAs from wild-type *Arabidopsis* inflorescences, leaves, seedlings, and siliques yielded 887,266 reads that matched the *Arabidopsis* genome (R.R. and D.P.B., unpublished data), of which 1,806 were *AtTAS3*-derived tasiRNAs. Many were in phase with the 3′ cleavage site, but a sizable proportion, particularly from the center and 5′ region of the locus, were not (Figure 2A). These alternatively phased siRNAs were largely in a register predicted by miR390-directed cleavage at the newly identified 5′ site. However, these alternatively phased siRNAs were almost equally consistent with the register that would be set by the most abundant *TAS3* siRNA, TAS3 5′D2(−) (Figure 2A). Because the newly identified 5′ miR390 complementary site in *AtTAS3* was unable to direct miR390-directed cleavage (see below), we favor the hypothesis put forward by Allen et al. (2005) that the alternatively phased *AtTAS3* tasiRNAs are phased by TAS3 5′D2(−)-mediated cleavage.

EST sequences representing *AtTAS3* homologs from diverse seed plants have two reported regions of nucleotide conservation: an ~42-nt region corresponding to the *AtTAS3* tasiRNAs that target *ARF3* and *ARF4* (tasi*ARF*s) and an ~21-nt region corresponding to the 3′ miR390 complementary site (Allen et al., 2005). We found a third conserved region of seed-plant *AtTAS3* homologs, which corresponded to the 5′ miR390 complementary site (Figure 2B), suggesting that dual targeting of tasiRNA precursors is an evolutionarily conserved function of miR390. For most of the *AtTAS3* homologs, cleavage at the 3′ miR390 complementary site would set the phasing register required for the accurate production of the two conserved tasi*ARF*s, which explains why the length of the region between tasi*ARF*s and the 3′ miR390 complementary site is relatively constant (Figure 2B; Allen et al., 2005). In contrast, the lengths of the regions between the newly identified 5′ miR390 complementary sites and the tasi*ARF*s were variable and generally out of phase with the tasi*ARF*s (Figure 2B). The exception was the sole gymnosperm *AtTAS3* homolog; for the loblolly pine (*Pinus taeda*) *TAS3* homolog, the 5′ miR390 complementary site was the one that was in the proper register for directing accurate production of the tasi*ARF*s, whereas the 3′ site was nine nucleotides out of phase.

Cleavage-Independent Function of a Conserved Plant miRNA Complementary Site

The 5′ miR390 complementary site of *AtTAS3* was unusual for a plant miRNA target in that it contained a mismatch and two G:U wobbles involving nucleotides 9–11 of miR390 (Figure 2A). Such mismatches in nucleotides surrounding the potential scissile phosphate inhibit miRNA-directed endonucleolytic cleavage in vitro and in vivo (Mallory et al., 2004; Schwab et al., 2005). Mismatches involving positions 9–11 of miR390 were a conserved feature of the 5′ sites of *TAS3* homologs and were in stark contrast to the pairing preferences for the 3′ sites of the same homologs (Figure 2C) and those observed for plant miRNA complementary sites in general (Mallory et al., 2004). 5′ RACE failed to detect cDNA ends terminating within the upstream site (data not shown), which suggested that the conserved, noncanonical 5′ miR390 complementary sites of flowering-plant *TAS3* genes might function independently of target cleavage.

We next tested, using wheat-germ extract (Tang et al., 2003), the biochemical properties of the miR390 complementary sites. A substrate containing the 5′ miR390 complementary site of a moss *TAS* gene (*PpTAS3*) was cleaved in vitro (Figure 3A). Similarly, the 5′ complementary site from the gymnosperm homolog (*PtTAS3*) was efficiently cleaved despite the presence of a mismatch at position 10 (Figure 3A). Cleavage at the *PtTAS3* 5′ site demonstrated that some cleavage targets could be missed when using target-prediction guidelines, such as those of Schwab et al. (2005), that forbid mismatches at position 10. In contrast, cleavage of the 5′ site of *AtTAS3*, which lacked Watson-Crick pairing at positions 9, 10, and 11, was not detected under conditions in which cleavage of the 3′ site was observed (Figures 3A and 3B). Mutations disrupting the 3′ site abolished cleavage, whereas adding additional miR390 to increase the amount of miR390-programed silencing specifically enhanced cleavage (Figure 3B). Repairing the mismatches to nucleotides 9–11 of miR390 resulted in efficient cleavage at the 5′ site, indicating that comparable cleavage of the wild-type 5′ site would have been detected had it occurred (Figure 3B).

Cleavage of the *PtTAS3* 5′ site provided an explanation for why the pine tasi*ARF*s were in phase with the 5′ miR390 complementary site rather than the 3′ site (Figure 2B); because the *PtTAS3* site can be cleaved, it could be the site that sets the phasing register for tasi*ARF* production in pine. As a corollary, the mismatches found in the 5′ site of *AtTAS3* and conserved among flowering plants appear to prevent cleavage that would set an inappropriate register for tasi*ARF* production from the *TAS3* genes of most flowering plants.

If the newly identified 5′ miR390 complementary site of *AtTAS3* evolved to interact with miR390 without being cleaved, we reasoned that it would efficiently bind the miR390-programmed silencing complex. To test this idea, we measured the ability of different sites to bind and act as competitive inhibitors of the endogenous silencing complex. Unlabeled RNA containing the *AtTAS3* 3′ site

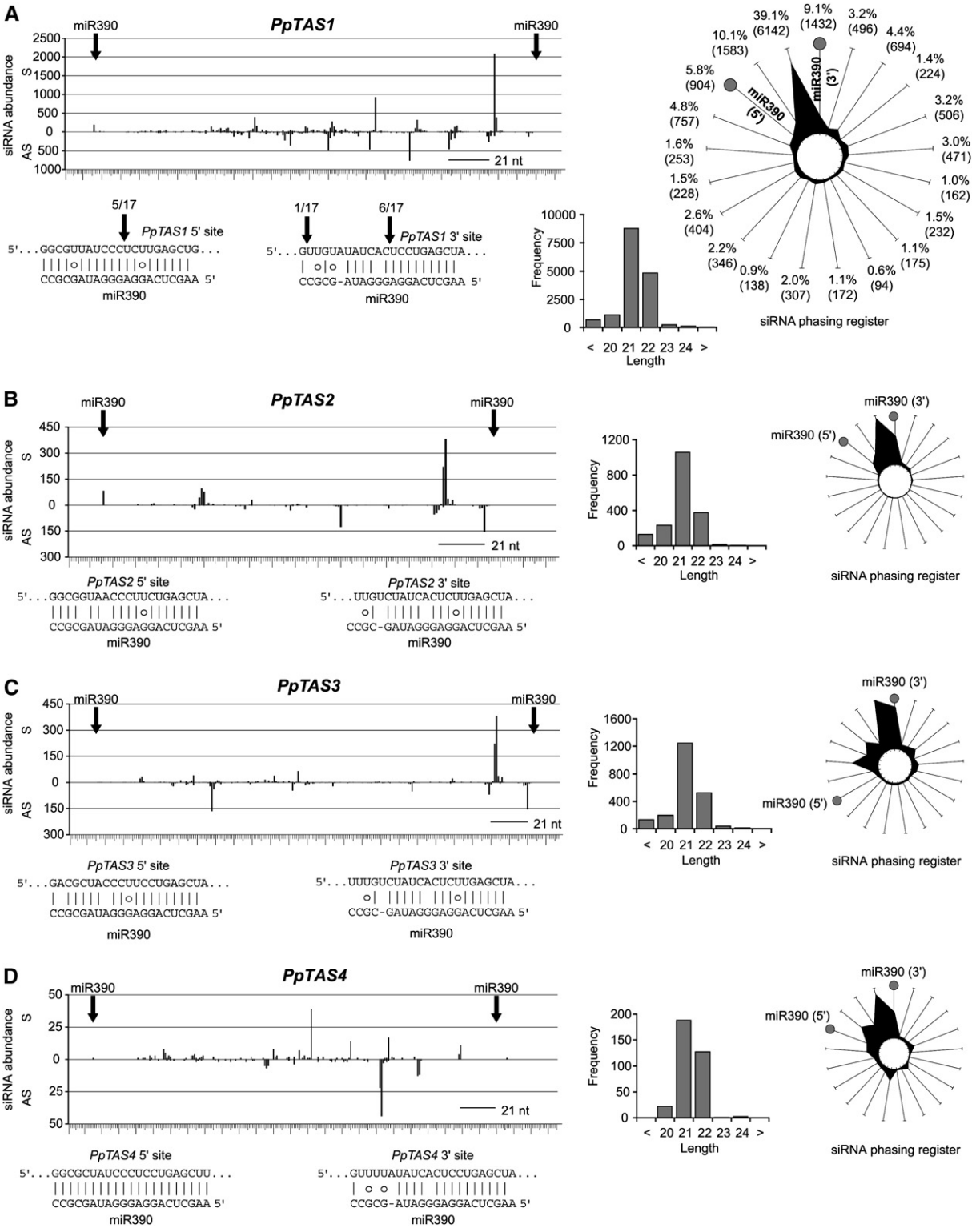

Figure 1. Phased *P. patens* siRNAs Mapped between miR390 Complementary Sites

(A) *PpTAS1*. The number of sequenced small RNAs with 5′ residues at each position along the *PpTAS1* locus is plotted for the sense (S) and antisense (AS) strands. The positions corresponding to the miR390 complementary sites are indicated by arrows, and pairing between the complementary sites and miR390 is shown below. The positions of 5′ ends mapped by RACE are indicated at the complementary sites by arrows, along with the fraction of sequenced clones mapping to the position. The length distribution and phasing of the small RNAs is plotted on the right. Each spoke of the radial

competed for cleavage of the identical labeled substrate with classical Michaelis-Menten behavior (K_m = 8.4 nM; k_{cat} = 0.006/s, estimating the concentration of endogenous miR390 silencing complex at 32 pM by quantitative northern). Adding *AtTAS3* 5′ site reduced the rate of cleavage even more efficiently, with the K_i of the 5′ site ~5-fold below the K_m of the 3′ site (Figure 3C). Disrupting complementarity to miR390 abolished the ability of both the 3′ and 5′ substrates to act as competitive inhibitors of miR390-mediated cleavage, thereby demonstrating the specificity of inhibition (Figure 3C). These observations, coupled with the conservation of central mismatches, indicated that the newly identified 5′ sites of flowering plants have evolved to bind the miR390 silencing complex while simultaneously avoiding cleavage. Indeed, analysis of flowering plant *AtTAS3* homologs showed that mismatches outside positions 8–11 were rare and almost never more disruptive than a G:U wobble (Figure 2C).

Both miR390 Complementary Sites Are Required for Full *AtTAS3* Function

We transformed *tas3-1*$^{-/-}$ plants with an *AtTAS3* genomic construct that can complement the *tas3-1* developmental defects (Adenot et al., 2006) and compared the frequency of complementation to that observed with variant constructs that had changes in one or both of the miRNA complementary sites (Figure 4). Of the primary transformant (T1) plants transformed with the wild-type *AtTAS3* construct (++), 37% were complemented for *AtTAS3* function, as indicated by lack of the elongated and curled leaves characteristic of the *tas3-1* line. Disrupting the 3′ complementary site (+Δ) lowered the frequency of complementation to 19.4%, demonstrating the importance of the 3′ site. Mutations of the 5′ complementary site that either disrupted binding (Δ+) or enhanced cleavage (R+) in vitro lowered the frequency of complementation to levels comparable to those of the 3′ site disruption. These results demonstrate the importance of binding without cleavage at this site, which was out of phase with the functional siRNAs. Simultaneous disruption of both sites (ΔΔ) lowered the apparent complementation frequency to 13.1%, a value indistinguishable from the background level of the assay. The lower complementation frequency of the ΔΔ construct compared with all constructs with single sites suggested some complementation by the single-site constructs, even the RΔ construct which contained a cleavable 5′ site and a disrupted 3′ site. We suspect that the relatively infrequent cases in which the single-site constructs complemented the *tas3-1* phenotype were due to miRNA-enhanced siRNA generation from the integrated transgene locus; transgenes often trigger siRNA production, especially when they include an miRNA complementary site (Parizotto et al., 2004), and the inventory of small RNAs produced from *TAS3* transgenes might occasionally include sufficient levels of tasi*ARF*s to enable wild-type development. Overall, the differential efficacies of the wild-type and single-site constructs demonstrate the importance of both miR390 complementary sites for *AtTAS3* function, and when considered together with our other results for the *AtTAS3* 5′ site, they indicate that an miRNA binding site that is not cleaved can nonetheless play an important, evolutionarily conserved role in plants.

A Conserved Trigger for siRNA Biogenesis

To test the hypothesis that dual small RNA complementary sites predispose the bounded region toward phased siRNA production, we examined *Arabidopsis* genes with multiple complementary sites for evidence of siRNA production. *ARF3* and *ARF4* both possess two sites complementary to the tasi*ARF*s TAS3 5′D7(+) and TAS3 5′D8(+) (Allen et al., 2005; Williams et al., 2005). For both *ARF3* and *ARF4*, our set of 887,266 *Arabidopsis* small RNA reads contained siRNAs from the region bounded by the tasi*ARF* complementary sites. These included 32 siRNA reads from the bounded region of *ARF4* and one read from the bounded region of *ARF3*. All 32 of the *ARF4* reads were in phase with each other (see Figure 5A and Figure S4), and the single *ARF3* read was in perfect phase with the cleavage sites (data not shown). For *ARF3*, no additional reads were observed outside of the bounded region, but for *ARF4*, an additional population of sense and antisense small RNAs arose from the region downstream of the 3′ complementary site. However, in contrast to the 21-nt, phased siRNAs from the region spanning the two sites, the siRNAs from the downstream cluster were not in phase with each other and were a mixture of 21-mers and 24-mers (Figure 5A). On the whole, the endogenous siRNAs from *ARF3* and *ARF4* supported the

graph represents 1 of the 21 possible phasing registers, with the total number of small RNAs mapping to that register plotted as distance from the center. The registers proceed clockwise from 5′ to 3′. The percentages and total number of sequenced siRNAs from each register are noted. The phasing registers of siRNAs from the antisense strand were corrected to account for the 2-nt, 3′ overhangs characteristic of Dicer-like cleavage. The specific registers predicted by 21-nt processing from the 5′ and 3′ cleavage sites are indicated with gray circles. Thus, phasing of the small RNA populations consistent with cleavage at one or the other site is indicated by abundant siRNAs that are in registers proximal to those predicted by the cleavage sites. For *PpTAS1*, 11,314 (72%) of the siRNAs were in phase with one of the complementary sites, in that they were in the same register or in immediately adjacent registers.

(B) *PpTAS2*, as in (A). The most populated register contained 709 siRNAs (39.1%); 1,648 (91%) of the siRNAs fell in the same or adjacent register(s) as a complementary site.

(C) *PpTAS3*, as in (A). The most populated register contained 524 siRNAs (24.3%); 1,097 (51%) of the siRNAs fell in the same or adjacent register(s) as a complementary site.

(D) *PpTAS4*, as in (A). The most populated register contained 80 siRNAs (23.3%); 221 (64%) of the siRNAs fell in the same or adjacent register(s) as a complementary site.

High-resolution graphs are also available (Figure S1).

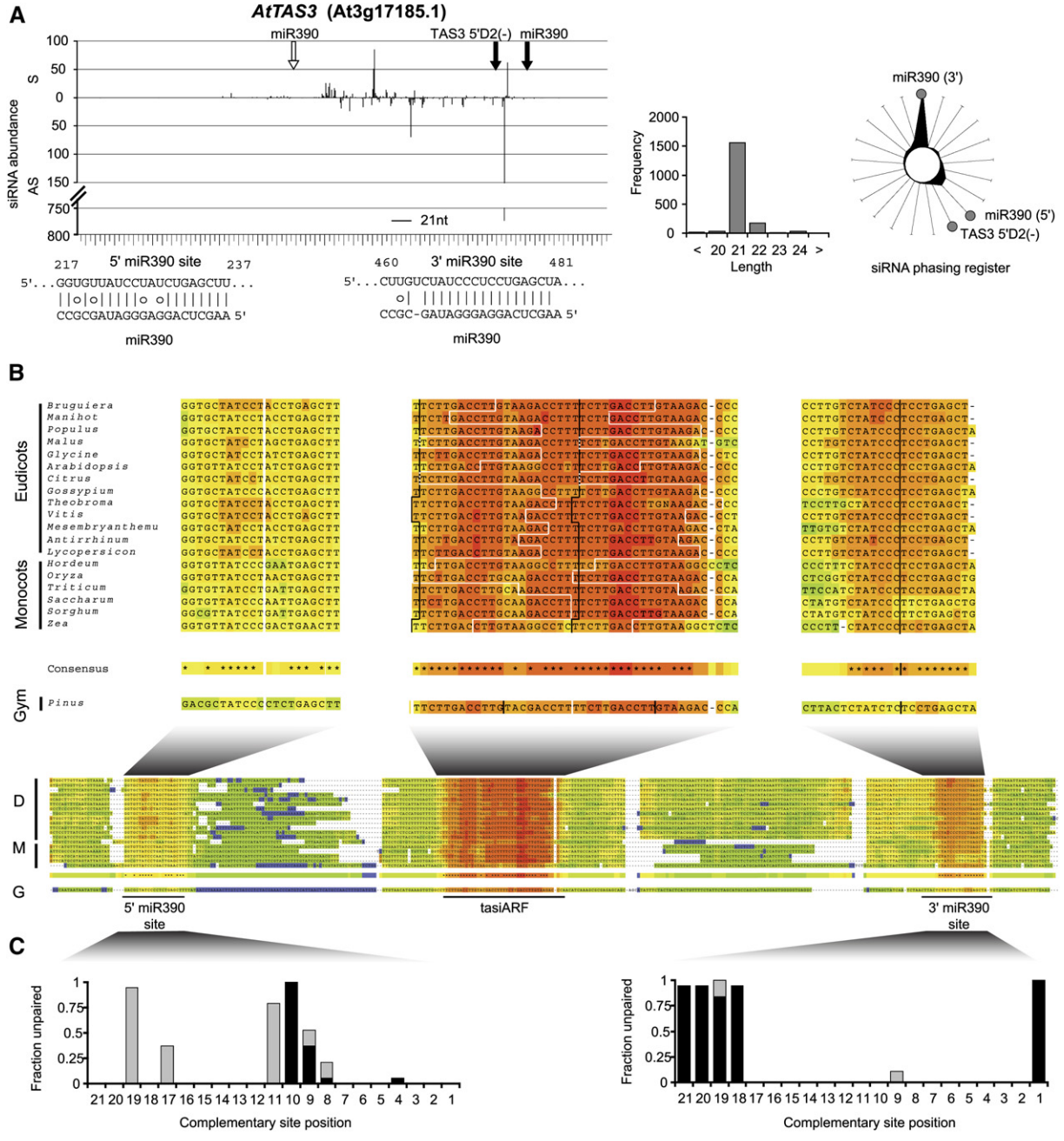

Figure 2. Dual miR390 Complementary Sites Were Conserved in Seed-Plant *TAS3* Loci

(A) *AtTAS3* siRNAs. The positions, length distribution, and phasing register of *Arabidopsis* small RNAs corresponding to *AtTAS3* are plotted as in Figure 1. A high-resolution graph is also available (Figure S1). The two miR390 complementary sites are indicated by arrows, with the open arrow indicating that no evidence of cleavage at the 5′ site was found. The site of secondary cleavage proposed to be directed by the highly abundant TAS3 5′D2(−) tasiRNA is also indicated (Allen et al., 2005). The most populated register contained 883 siRNAs (48.5%); 1,440 (79%) of the siRNAs fell in the same or adjacent register(s) as a complementary site.

(B) *TAS3* ESTs from diverse flowering plant genera contained dual miR390 complementary sites that flank the area of predicted tasiRNA production. Alignments were generated using ClustalW and color-coded based on the confidence of the local alignment using the CORE function of T-Coffee. tasi*ARF* refers to the regions homologous to *AtTAS3* 5′D7(+) and *AtTAS3* 5′D8(+). The regions corresponding to the 5′ miR390 complementary site, tasi*ARF*, and the 3′ miR390 complementary site are expanded. Black and white lines indicate the registers in phase with the 3′ and 5′ sites, respectively. EST details are given in Table S2. Gym, Gymnosperm.

(C) Analysis of miR390 complementary sites in EST homologs of *AtTAS3*. Complementary site positions were numbered starting with the residue corresponding to the 5′ nucleotide of miR390 and scored based on their pairing to *Arabidopsis* miR390a. Gray, G:U wobbles; black, other non-Watson-Crick pairs. This analysis was restricted to the flowering-plant *TAS3* homologs because the 5′ site of the *Pinus taeda* homolog is cleaved.

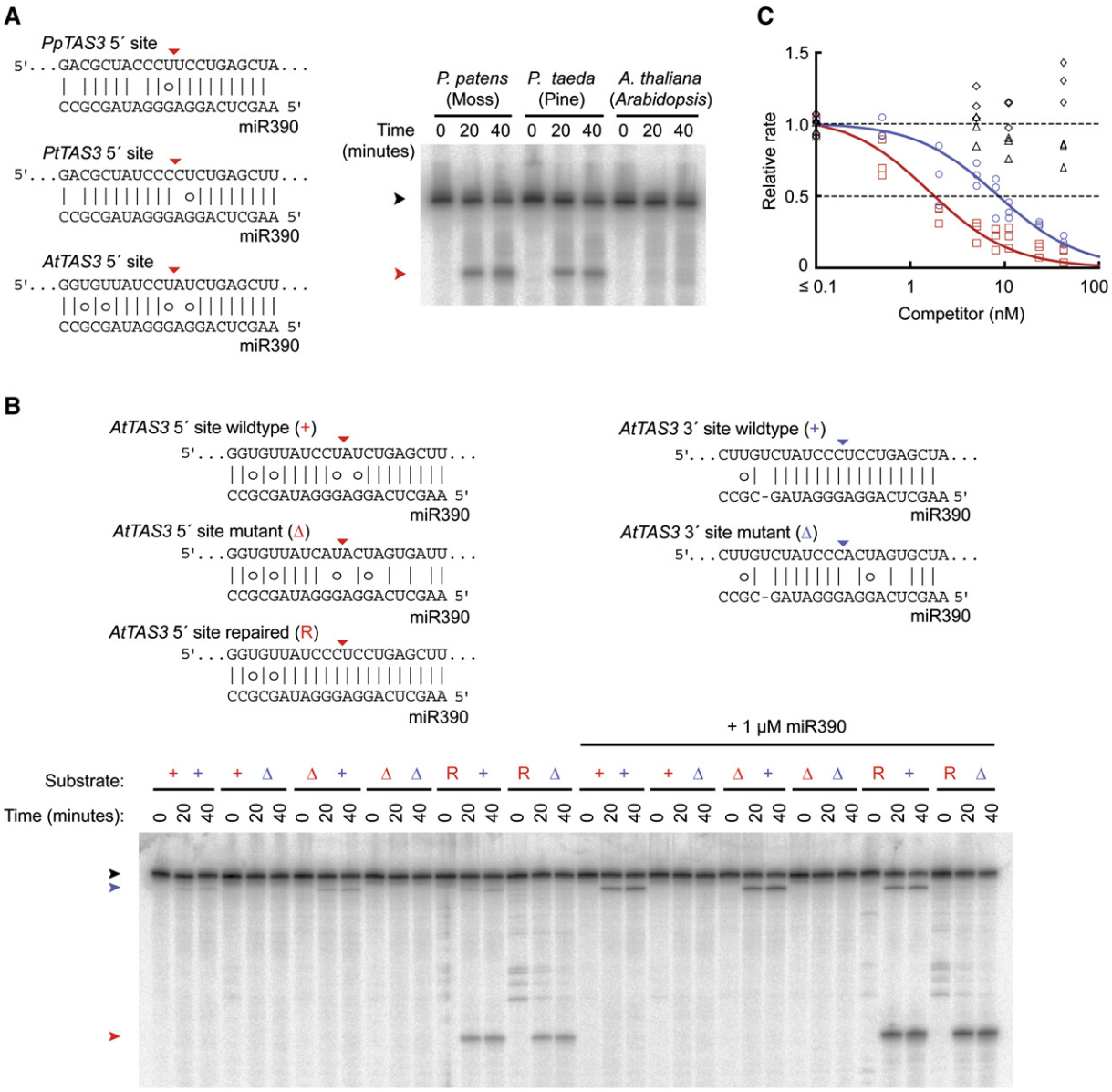

Figure 3. A Cleavage-Independent miRNA-Target Interaction in Flowering Plants

(A) miR390-directed cleavage of a target with a mismatch at position 10, but not one with a mismatch flanked by two G:U wobbles. The 5′ complementary site of *AtTAS3* was changed to the indicated sequences to mimic the sites found in *P. patens TAS3* or *P. taeda TAS3*. Cap-labeled RNAs containing only the 5′ complementary site were incubated with miR390-programmed wheat-germ lysate for the indicated times. Black and red arrowheads indicate the positions of uncut and cleaved substrate, respectively.

(B) The 5′ miR390 site of *AtTAS3* resisted miR390-mediated cleavage because of conserved mismatches at positions 9–11. Cap-labeled *AtTAS3* RNA encompassing both sites was incubated for the indicated times with wheat-germ lysate, with or without supplemental miR390. The sequences of 5′ and 3′ complementary site variants are shown paired to miR390. Red, 5′ site; blue, 3′ site; +, wild-type; Δ, disruptive mutation; R, repaired site. The positions of RNAs cleaved at the 3′ and 5′ site are indicated with blue and red arrowheads, respectively, while uncleaved substrate RNA is indicated by a black arrowhead.

(C) The cleavage-refractory 5′ miR390 complementary site of *AtTAS3* was a potent inhibitor of miR390-mediated cleavage. The relative rates of in vitro target cleavage using 1 nM of radiolabeled *AtTAS3*-derived RNA containing only the wild-type 3′ complementary site as substrate are plotted with varying concentrations of unlabeled RNA containing the wild-type 3′ site (blue circles), the wild-type 5′ site (red squares), the disrupted 3′ site (black triangles), or the disrupted 5′ site (black diamonds). The blue line shows the best fit to the data for the wild-type 3′ site and indicates a K_m for this site of 8.4 nM, whereas the red line shows the best fit to the data for the wild-type 5′ site and indicates a K_i for this site of 1.4 nM.

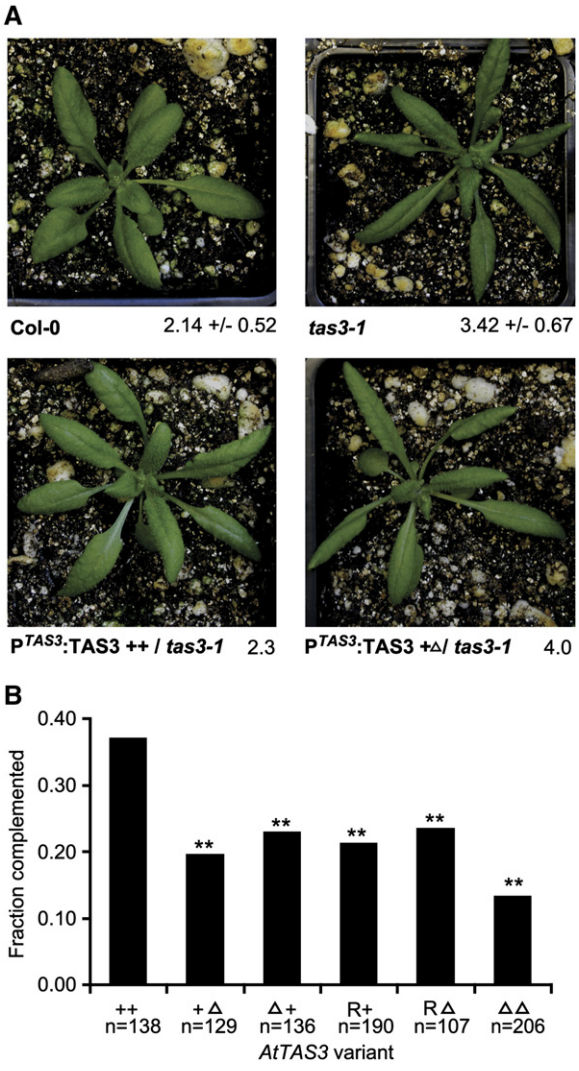

Figure 4. Dual miR390 Complementary Sites Are Required for Full *AtTAS3* Function

(A) Representative *tas3-1* transformants. The mean and standard deviation of the length to width ratio of the sixth leaf is reported for Col-0 (n = 40) and *tas3-1* (n = 41) control plants. Transformants with a ratio of less than 2.7 were scored as complementing (example at lower left), while those with ratios higher than 2.7 were scored as noncomplementing (example at lower right).

(B) The fraction of complemented *tas3-1* primary transformants after transformation with the indicated variants of *AtTAS3*. The number (n) of independent T1 plants examined for each variant is listed below. The sequences of 5′ and 3′ site variants are as in Figure 3. All statistically significant differences from the wild-type, as evaluated based on Chi-square goodness-of-fit tests, are indicated (**p < 0.01).

hypothesis that dual small RNA-mediated cleavage events predispose the intervening fragment toward recognition by an RdRp, leading to the production of phased siRNAs.

Several repetitive pentatricopeptide repeat (*PPR*) genes have been predicted or validated as targets of miR161, miR400, and *AtTAS1b*- and *AtTAS2*-derived tasiRNAs (Rhoades et al., 2002; Allen et al., 2004, 2005; Sunkar and Zhu, 2004; Vazquez et al., 2004a). We found 15 *PPR* genes that had at least two sites complementary to miR161.1, miR400, TAS1b 3′D4(−), or TAS2 3′D6(−). All 15 of these genes, including *At1g62670*, which was recently reported to give rise to secondary siRNAs (Ronemus et al., 2006), produced siRNAs from between small RNA complementary sites (Figure 5B and Figures S2 and S4). The *PPR*-associated siRNA populations were predominantly 21 nt in length, with a small proportion being 22 nt. Because of the highly repetitive nature of these target genes, many of the siRNAs could not be assigned to a single locus; however, even with this complication, the majority of the *PPR*-derived siRNAs were in a 21-nt phase at registers consistent with cleavage at known or predicted target sites, with 58% beginning within one nucleotide of the one predicted by cleavage at one of the sites (Figure 5B and Figures S2 and S4). This represents a substantial enrichment of phased siRNAs when compared with a random distribution of small RNAs falling into each of the possible 21 registers.

Analyses of secondary siRNAs deriving from miRNA targets with a single complementary site underscored the importance of dual complementary sites. Very little evidence of the production of siRNAs from single-site miRNA targets has been reported, with only the targets of miR168, miR393, and miR408 generating small RNAs that have been detected by sequencing of *Arabidopsis* small RNAs (Lu et al., 2005; Ronemus et al., 2006). The very low abundance of secondary siRNAs corresponding to *Arabidopsis* miRNA targets was also observed when we analyzed our large set of sequenced *Arabidopsis* small RNAs: as previously reported, significant numbers of secondary siRNAs were derived from *AGO1*, the only known target of miR168, as well as from the targets of miR393 (Figures S3 and S4). Sense and antisense small RNAs, predominantly 21 nt in length, arose only from the region downstream of the miRNA complementary sites, and they tended to be in phase with the end defined by miRNA-mediated cleavage (Figures S3 and S4). The phasing register, sizes, and downstream location of these secondary siRNAs were reminiscent of *AtTAS1a-c* and *AtTAS2* tasiRNAs, suggesting that they may have arisen through a common mechanism. Nonetheless, these examples were exceptions to the general observation that plant miRNA targets with single miRNA complementary sites were not efficient substrates for RdRp activity and subsequent production of secondary siRNAs. Even deeper sequencing of *Arabidopsis* small RNA populations may reveal that siRNA formation from single-site miRNA targets is a more widespread, albeit very low-efficiency, phenomenon. Taken together, our results strongly support a model in which dual miRNA complementary sites consistently predispose the bounded region of the target toward entry into a tasiRNA-like pathway, whereas a single miRNA complementary site triggers siRNA production less reliably and less efficiently.

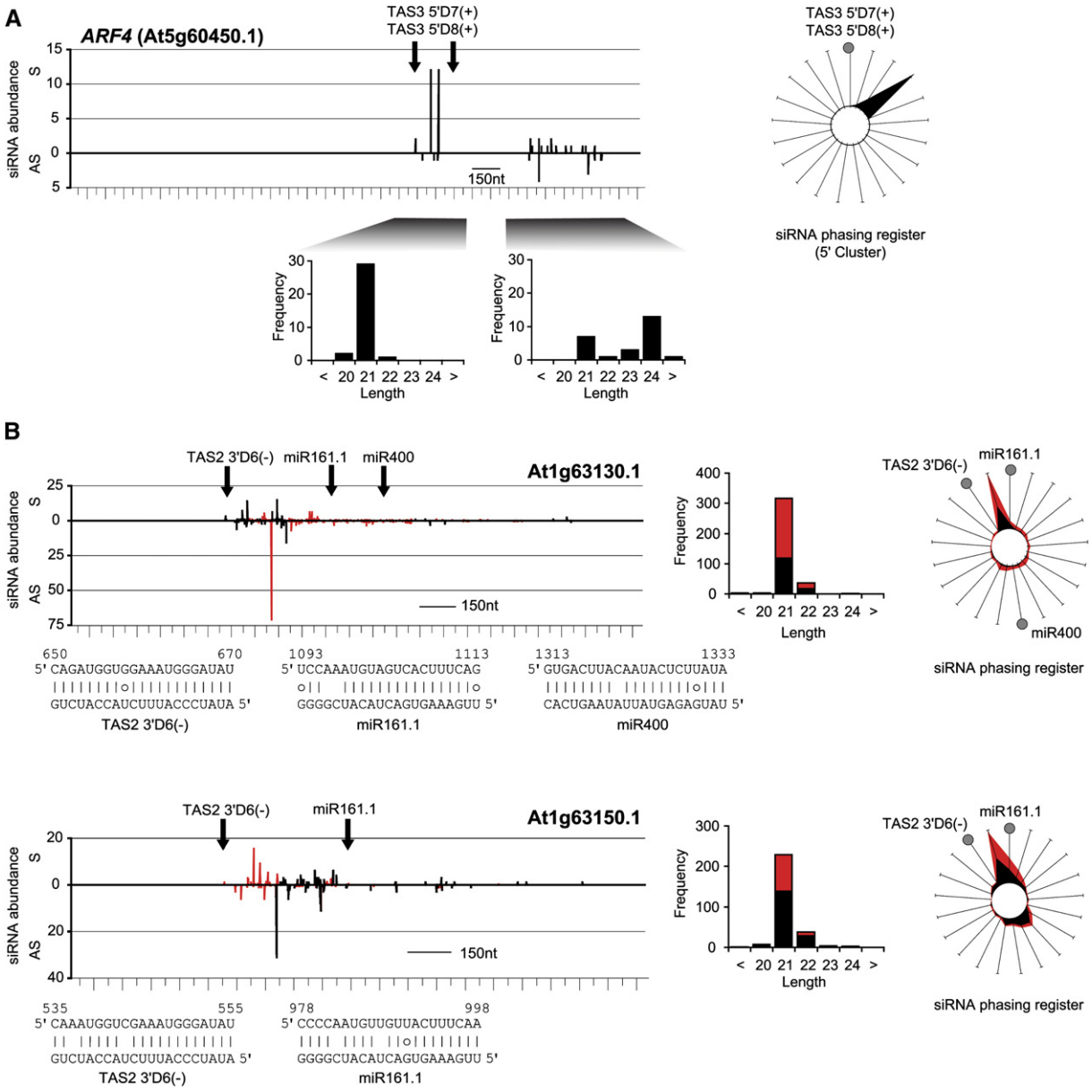

Figure 5. Multiple Small RNA Complementary Sites Correlate with siRNA Production from *Arabidopsis* Genes

(A) The positions, length distribution, and phasing register of *Arabidopsis* small RNAs corresponding to *ARF4* mRNA are plotted as in Figure 1. The most populated register contained 26 siRNAs (81.3%). The positions within the mRNA of the complementary sites to the tasi*ARF*s TAS3 5′D7(+) and TAS3 5′D8(+) RNAs are indicated by black arrows. The length distributions of two distinct clusters of *ARF4*-derived small RNAs are indicated separately.

(B) Small RNAs corresponding to the *PPR* mRNAs *At1g63130.1* and *At1g63150.1* are plotted as in (A). Complementary sites for miR161.1, miR400, and TAS2 3′D6(−) are indicated by arrows and displayed below. Small RNAs that matched only one site in the *Arabidopsis* genome are represented by black, whereas small RNAs with more than one match to the genome are plotted in red, after being normalized for the number of matching loci (e.g., a sequence with three reads that matches the genome twice would contribute 1.5 counts to each locus). The most populated register for *At1g63130.1* contained 96 (43.3%) unique and 78 (56.1%) ambiguous siRNAs; 118 (85%) of the unique and 149 (67%) of the ambiguous siRNAs fell in the same or adjacent register(s) as a complementary site. The most populated register for *At1g63150.1* contained 41 (39.9%) unique and 44 (24.6%) ambiguous siRNAs; 92 (51%) of the unique and 70 (68%) of the ambiguous siRNAs fell in the same or adjacent register(s) as a complementary site. The 13 other *PPR* genes with multiple small RNA complementary sites also gave rise to phased siRNAs (Figure S2).

DISCUSSION

One of the first reports on tasiRNAs noted their ~21-nt phasing, which was suggestive of successive DCL-catalyzed cleavage beginning from a defined point on a dsRNA substrate (Vazquez et al., 2004b). It was subsequently recognized that the single-stranded tasiRNA precursors are cleaved by miRNAs (Allen et al., 2005; Yoshikawa et al., 2005), and that this cleavage site defines a starting point for DCL4-catalyzed siRNA processing (Gasciolli et al., 2005; Xie et al., 2005). Yet the majority of *Arabidopsis* miRNA targets are cleaved without subsequently initiating the biogenesis of detectable amounts of siRNAs (Lu et al., 2005). What molecular features allow a plant cell to discriminate between the minority of cleavage products that are efficiently converted to siRNAs and the majority that are not? In the case of the siRNAs triggered by miR390, the expressed siRNAs emanate from a region flanked by miR390 complementary sites. The phasing registers of the *PpTAS* siRNA populations (Figure 1) and the observation of miR390-directed cleavage at both complementary sites in *PpTAS1* (Figure 1A) were consistent with successive DCL activity initiated from both ends of a dsRNA whose termini were defined by dual miR390-mediated cleavage events. The location of the pine tasi*ARF*s, which also appeared to be flanked by two cleavable sites (Figure 2B and Figure 3A), suggested that the same process produces siRNAs in gymnosperms. Furthermore, phased siRNAs were universally observed to emanate from regions of *Arabidopsis* genes bounded by small RNA complementary sites (Figure 5 and Figures S2 and S4). Small RNAs whose 5′ ends were within one nucleotide of the residues predicted by successive cleavage in precise 21-nt increments account for 71% of all small RNAs observed from *P. patens* and *Arabidopsis* genes with two or more complementary sites, indicating that such loci produced phased siRNAs. Precise 21-nt phasing appears to have degenerated as a result of occasional 22-nt cleavages, as indicated by the occurrence of both 21- and 22-nt small RNAs; otherwise, the fraction in phase would have been even higher. We conclude that one discriminating molecular feature of an RNA that triggers RdRp activity and subsequent entry into a phased siRNA pathway is the occurrence of dual small RNA-mediated cleavage events. Perhaps the resulting lack of any molecular signatures of normally processed mRNA (i.e., lack of 5′ cap, 3′ poly-A tail, and other mRNA-associated factors such as those deposited during splicing) direct such dual cleavage products to become RdRp substrates (Figure 6A).

AtTAS3 also contains dual miR390 complementary sites, the importance of which was highlighted by their conservation during seed-plant evolution and their requirement for efficient complementation of *tas3* plants (Figures 2–4). The observation that tasiRNAs from such a wide breadth of plant lineages derive from loci falling between miR390 complementary sites suggests an ancient and broadly conserved hallmark of siRNA biogenesis. Curiously, the 5′ miR390 complementary sites of flowering plant *TAS3* loci consistently contained mismatches to miR390 at positions critical for target cleavage (Figure 2C). These conserved mismatches at the center of the complementary site prevented miR390-mediated cleavage in vitro, yet they permitted efficient binding (Figure 3). Taken together, these results indicate that this site functions independent of target cleavage in initiating production of *AtTAS3* tasiRNAs (Figure 6B). We suggest that there might be additional instances in which miRNA binding without cleavage could have important functions in plants.

Dual miRNA complementary sites are an ancient trigger for siRNA biogenesis, but they are not the only trigger. *AtTAS1a-c* and *AtTAS2* precursors are cleaved at a single site upstream of the segment converted to siRNAs (Allen et al., 2005). Similarly, some other singly-cleaved *Arabidopsis* miRNA targets give rise to siRNAs from the area downstream of miRNA-mediated cleavage (Lu et al., 2005; Ronemus et al., 2006; Figures S3 and S4). We considered the possibility that these or other *Arabidopsis* miRNA targets might possess a second, previously unrecognized, miRNA complementary site. Even after drastically relaxing the stringency of target-site prediction to a level where past efforts have been unable to distinguish signal from noise, we found potential second sites in only 3 of 77 targets for which cleavage has been validated; none of the 3 were in *AtTAS1a-c*, *AtTAS2*, or the targets of miR168 and miR393 (data not shown). Thus, we conclude that there are very few, if any, unknown second sites among the currently known miRNA targets. What might replace the downstream miRNA complementary site and act as the second hit to trigger siRNA biogenesis from a few of these loci? Perhaps these transcripts have another mechanism for downstream cleavage involving another type of ribonuclease. Alternatively, downstream cleavage might be bypassed; in principle, RDR6 could be recruited to these transcripts by some other means; e.g., through a downstream binding element (Figure 6C). We note that in each of these cases (*AtTAS1a-c*, *AtTAS2*, and the targets of miR168 and miR393), the miRNA itself cannot be acting as a primer for RDR6-mediated RNA polymerization because all sequenced siRNAs arise exclusively from the 3′ region of the miRNA complementary site.

Production of siRNAs upstream of a single miRNA complementary site has been observed for a highly transcribed gene designed to be an miRNA "sensor" (Parizotto et al., 2004). Our hypothesis points to a possible mechanism for how such upstream siRNAs might be triggered. Perhaps a rare, upstream nonspecific cleavage, coupled with efficient miRNA-mediated processing, defines an initial RDR6 template in much the same way as dual miRNA-mediated cleavage does (Figure 6D). Because the miRNA sensor is highly expressed, initial siRNAs would likely encounter additional transcripts and direct their cleavage upstream of the miRNA complementary site, thereby generating more RDR6 substrates and initiating a cascade that results in the repression of the

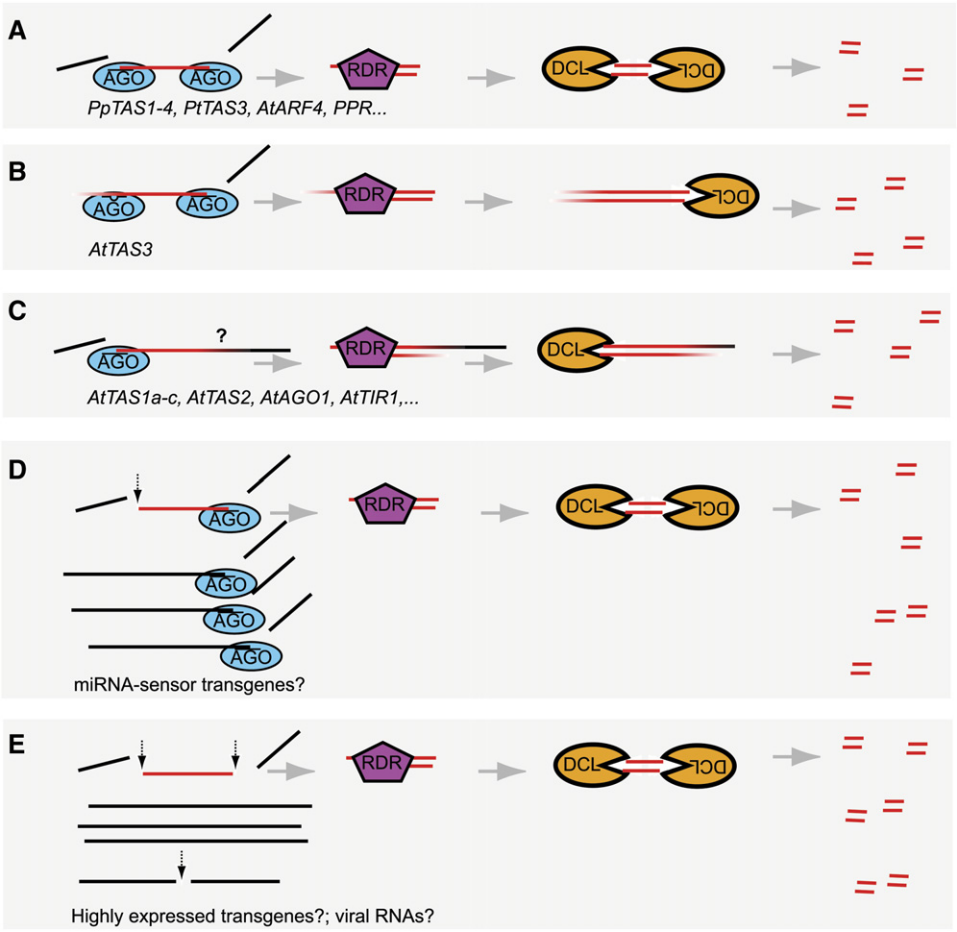

Figure 6. Different Embodiments of the Two-Hit Model for siRNA Biogenesis in Plants

(A) The internal product of dual miRNA- or siRNA-directed cleavage is recognized as a substrate for RdRp activity, which produces a dsRNA with two well-defined ends, as for *PpTAS1-4*, *PtTAS3*, *AtARF4*, and many *PPR* genes. Subsequent processing by a DCL enzyme produces populations of siRNAs in phase with one or the other end.

(B) The segment of an RNA flanked by miRNA complementary sites, only one of which is competent for AGO-catalyzed cleavage, defines an RdRp substrate, as in *AtTAS3*. Subsequent DCL processing of this dsRNA proceeds chiefly from the terminus defined by the miRNA-mediated cleavage.

(C) The segment of RNA defined on the 5′ by miRNA-directed cleavage and defined on the 3′ by an unknown element (question mark) that helps recruit RdRp activity gives rise to dsRNA, as in *AtTAS1a-c*, *AtTAS2*, and a limited number of other miRNA targets (Figure S3). Subsequent DCL processing of the dsRNA proceeds chiefly from the terminus defined by the miRNA-mediated cleavage.

(D) The segment of a very abundant RNA defined on the 5′ by a very rare, random cleavage event and defined on the 3′ by miRNA-directed cleavage becomes recognized as an RdRp substrate. This mechanism may trigger silencing of miRNA-sensor transgenes in plants.

(E) The segment of a very abundant RNA defined by two rare, random cleavage events becomes recognized as a substrate for RdRp activity. This mechanism may trigger transgene and virus silencing.

High-resolution graphs are also available (Figure S4).

sensor. Indeed, the probability of rare, nonspecific RNA cleavage occurring twice on the same mRNA molecule will increase as the abundance of that mRNA increases. For very highly expressed messages, such as those from viruses or transgenes, random nonspecific cleavage events might generate a few fragments that lack both a 5′ cap and a 3′ poly-A tail (Figure 6E). If, as our observations suggest, this type of RNA fragment is efficiently recognized by the *RDR6/DCL4* pathway, the resulting siRNAs would target other copies of the highly expressed transcript, facilitating the formation of more fragments without caps and tails and initiating a cascade that ultimately silences the virus or transgene. We note that this model postulates that the triggers for tasiRNA biogenesis and siRNA-mediated virus resistance are mechanistically similar—a postulate supported by the fact that a single Dicer-like protein, DCL4, is primarily responsible for both processes in wild-type *Arabidopsis* (Gasciolli et al., 2005; Xie et al., 2005; Yoshikawa et al., 2005; Bouche et al., 2006; Deleris et al., 2006). This two-hit model also

provides a molecular mechanism that rationalizes threshold models proposed previously to explain the observation that high initial expression levels of transgenes correlate with high frequencies of silencing initiation (Lindbo et al., 1993; Smith et al., 1994; Elmayan and Vaucheret, 1996). In our model, the plant cell detects over-abundant mRNA species because more abundant transcripts have a greater chance of both triggering and propagating the silencing cascade, i.e., more abundant species are more likely to include spontaneously generated fragments lacking both caps and tails, and more abundant species are more likely to be targeted by the resultant siRNA molecules, which in turn helps to generate more fragments lacking both caps and tails. The two-hit hypothesis thus outlines a mechanistic model for the initial identification of aberrant/dangerous RNA by the silencing machinery, and further suggests that the triggering of siRNA production can be directed to less abundant transcripts by the presence of dual miRNA complementary sites, which appears to have been occurring for the miR390-targeted *TAS* loci for the past 400 million years.

EXPERIMENTAL PROCEDURES

RNA Extractions

Total RNA from *P. patens* was isolated from three wild-type samples cultivated on minimal media agar overlaid with cellophane discs under standard conditions: Protonemata (7 day culture, 22°, 16 hr light), protonemata + young gametophores (14 day culture, 22°, 16 hr light), and gametophore + sporophytes (on media lacking NH_4-tartarate; 21 days at 22°, 16 hr light, followed by transfer to 15°, 8 hr light, with irrigation, for 39 days). Specimens were ground in 100 mM Tris-HCl (pH 9.0), 2% hexadecyltrimethylammonium bromide, 0.5% SDS, 2% polyvinyl pyrrolidone 40, 5 mM EDTA, and 10 mM β-mercaptoethanol. Samples were then phenol/chloroform extracted, ethanol precipitated, resuspended in 250 mM NaCl, and placed on ice for 20 min to precipitate carbohydrates. After centrifugation, the supernatant was ethanol precipitated to recover total RNA.

Small RNA Sequencing and Data Analysis

Construction of small RNA cDNA libraries was performed as described (Lau et al., 2001) and adapted for pyrosequencing (Supplemental Experimental Procedures). After phenol/chloroform extraction and native PAGE purification, 5 μg of purified PCR products for each library was delivered to 454 Life Sciences (Branford, CT, USA) for pyrosequencing. After discarding small RNAs that matched the *P. patens* chloroplast genome or the sense polarities of the nuclear 5S, 5.8S, 18S, or 26S rRNAs, the sequenced small RNAs were matched to the ~5.4 million *P. patens* WGS traces available at the time of analysis. Matching RNAs were classified as repetitive or nonrepetitive (Table S1, Supplemental Experimental Procedures). *PpTAS1-4* were found by using an algorithm that searched for clusters of nonrepetitive small RNAs from both the sense and antisense strand of WGS traces in which a significant fraction of the small RNAs were in phase with each other (in the same or adjacent registers, accounting for the 2-nt offset expected between the sense and antisense strands). Homologs of *AtTAS3* (Figure 2B, Table S2) were found by searching the est_others database for EST sequences that contained a sequence highly similar to 5′- TTCT TGACCTTGTAAGGCCTTTTCTTGACCTTGTAAGACCCC-3′ (representing the two tasi*ARF*s).

5′-RACE

Cleaved transcripts were detected using 5′-RACE (Llave et al., 2002).

Oligonucleotides

Oligos used for library preparation, RACE, mutagenesis, and transcription are listed in the Supplemental Experimental Procedures.

In Vitro Assays

Wheat-germ extract was prepared as previously described (Tang et al., 2003). Templates for in vitro transcription were made by PCR from constructs used for *tas3-1* complementation (pART27-*AtTAS3*; Adenot et al., 2006). All RNAs were gel-purified, and substrate RNA was radiolabeled by capping using guanylyl transferase (Ambion, Houston, TX) and α-^{32}P GTP. Cleavage reactions contained 50% wheat-germ extract (v/v), 5 mM DTT, 0.1 U/μl RNasin (Promega), 25 mM phosphocreatine, 1 mM ATP, 40 mM KOAc, and 0.03 μg/μl creatine kinase. Extract was incubated with buffer ± 1 μM phosphorylated miR390 for 20 min at 26°C, then added to 10,000 cpm of RNA (~5 fmol) per reaction. Reactions were stopped by the addition of 25 volumes of TRI reagent (Ambion, Houston, TX) at the indicated time points, followed by RNA extraction and PAGE analysis. For competition assays, extract was preincubated for 10 min at 26°C and added to labeled substrate (1 nM final) premixed with unlabeled competitor. Percent cleavage was calculated as the density of the cleaved band divided by the sum of the densities of the cleaved and full-length bands, and initial rates were calculated by regression. For 3′ wild-type competition, data were fit to the Michaelis-Menten equation, correcting for the fraction of total RNA that was radiolabeled: $V_{obs} = (1\ nM / 1\ nM + X\ nM) \times (v_{max} \times [1 + X]\ nM) / (K_m + [1 + X]\ nM)$, where X is the concentration of unlabeled 3′ wild-type competitor. For 5′ wild-type competition, data were fit for competitive inhibition: $V_{obs} = (v_{max} \times 1\ nM) / (K_m \times (1 + X/K_i) + 1\ nM)$, where X is the concentration of the unlabeled 5′ wild-type competitor.

tas3-1 Complementation

Variants of pART27-*AtTAS3* (Figure 3B) were produced using QuickChange mutagenesis (Stratagene, La Jolla, CA) and transformed into *tas3-1* plants (Adenot et al., 2006). After 23–26 days of growth at ~22° in 16 hr light, 8 hr dark, the length-to-width ratio of the sixth rosette leaf was determined for each transformant. Nontransformed wild-type and *tas3-1* plants gave ratios of 2.14 ± 0.52 and 3.42 ± 0.67, respectively. Therefore, we classified transformants as "complementing" if this ratio was less than 2.7, recognizing that 17% of nontransformed *tas3-1* plants also scored as complemented, which represents the background of the assay.

Supplemental Data

The Supplemental Data for this article can be found online at http://www.cell.com/cgi/content/full/127/3/565/DC1/.

ACKNOWLEDGMENTS

We thank the Joint Genome Institute for the availability of *P. patens* WGS traces, Mitsuyasu Hasebe for the gift of *P. patens* spores and protocols, Herve Vaucheret for sharing the *tas3-1* homozygous line and pART27-*AtTAS3* construct prior to publication, Wendy Johnston for technical assistance, Guiliang Tang for advice on wheat-germ assays, and Matt Jones-Rhoades for computational assistance. This work was supported by a grant from the NIH, the Prix Louis D. from the Institut de France (D.P.B.), a Helen Hay Whitney Postdoctoral Fellowship (M.J.A.), and an NSF predoctoral fellowship (C.J.).

Received: March 21, 2006
Revised: July 7, 2006
Accepted: September 25, 2006
Published: November 2, 2006

REFERENCES

Adenot, X., Elmayan, T., Lauressergues, D., Boutet, S., Bouche, N., Gasciolli, V., and Vaucheret, H. (2006). DRB4-dependent *TAS3 trans*-acting siRNAs control leaf morphology through AGO7. Curr. Biol. *16*, 927–932.

Allen, E., Xie, Z., Gustafson, A.M., Sung, G.H., Spatafora, J.W., and Carrington, J.C. (2004). Evolution of microRNA genes by inverted duplication of target gene sequences in *Arabidopsis thaliana*. Nat. Genet. *36*, 1282–1290.

Allen, E., Xie, Z., Gustafson, A.M., and Carrington, J.C. (2005). microRNA-directed phasing during trans-acting siRNA biogenesis in plants. Cell *121*, 207–221.

Arazi, T., Talmor-Neiman, M., Stav, R., Riese, M., Huijser, P., and Baulcombe, D.C. (2005). Cloning and characterization of micro-RNAs from moss. Plant J. *43*, 837–848.

Axtell, M.J., and Bartel, D.P. (2005). Antiquity of microRNAs and their targets in land plants. Plant Cell *17*, 1658–1673.

Bartel, D.P. (2004). MicroRNAs: genomics, biogenesis, mechanism, and function. Cell *116*, 281–297.

Bouche, N., Lauressergues, D., Gasciolli, V., and Vaucheret, H. (2006). An antagonistic function for *Arabidopsis* DCL2 in development and a new function for DCL4 in generating viral siRNAs. EMBO J. *25*, 3347–3356.

Deleris, A., Gallego-Bartolome, J., Bao, J., Kasschau, K.D., Carrington, J.C., and Voinnet, O. (2006). Hierarchical action and inhibition of plant Dicer-Like proteins in antiviral defense. Science *313*, 68–71.

Elmayan, T., and Vaucheret, H. (1996). Expression of single copies of a strongly expressed *35S* transgene can be silenced post-transcriptionally. Plant J. *9*, 787–797.

Fahlgren, N., Montgomery, T.A., Howell, M.D., Allen, E., Dvorak, S.K., Alexander, A.L., and Carrington, J.C. (2006). Regulation of *AUXIN RESPONSE FACTOR3* by *TAS3* ta-siRNA affects developmental timing and patterning in *Arabidopsis*. Curr. Biol. *16*, 939–944.

Garcia, D., Collier, S.A., Byrne, M.E., and Martienssen, R.A. (2006). Specification of leaf polarity in *Arabidopsis* via the *trans*-acting siRNA Pathway. Curr. Biol. *16*, 933–938.

Gasciolli, V., Mallory, A.C., Bartel, D.P., and Vaucheret, H. (2005). Partially redundant functions of *Arabidopsis* DICER-like enzymes and a role for DCL4 in producing *trans*-acting siRNAs. Curr. Biol. *15*, 1494–1500.

Hunter, C., Willmann, M.R., Wu, G., Yoshikawa, M., de la Luz Gutierrez-Nava, M., and Poethig, R.S. (2006). Trans-acting siRNA-mediated repression of ETTIN and ARF4 regulates heteroblasty in *Arabidopsis*. Development *133*, 2973–2981.

Lau, N.C., Lim, L.P., Weinstein, E.G., and Bartel, D.P. (2001). An abundant class of tiny RNAs with probable regulatory roles in *Caenorhabditis elegans*. Science *294*, 858–862.

Lindbo, J.A., Silva-Rosales, L., Proebsting, W.M., and Dougherty, W.G. (1993). Induction of a highly specific antiviral state in transgenic plants: Implications for regulation of gene expression and virus resistance. Plant Cell *5*, 1749–1759.

Llave, C., Xie, Z., Kasschau, K.D., and Carrington, J.C. (2002). Cleavage of *Scarecrow-like* mRNA targets directed by a class of *Arabidopsis* miRNA. Science *297*, 2053–2056.

Lu, C., Tej, S.S., Luo, S., Haudenschild, C.D., Meyers, B.C., and Green, P.J. (2005). Elucidation of the small RNA component of the transcriptome. Science *309*, 1567–1569.

Mallory, A.C., Reinhart, B.J., Jones-Rhoades, M.W., Tang, G., Zamore, P.D., Barton, M.K., and Bartel, D.P. (2004). MicroRNA control of *PHABULOSA* in leaf development: importance of pairing to the microRNA 5′ region. EMBO J. *23*, 3356–3364.

Margulies, M., Egholm, M., Altman, W.E., Attiya, S., Bader, J.S., Bemben, L.A., Berka, J., Braverman, M.S., Chen, Y.J., Chen, Z., et al. (2005). Genome sequencing in microfabricated high-density picolitre reactors. Nature *437*, 376–380.

Parizotto, E.A., Dunoyer, P., Rahm, N., Himber, C., and Voinnet, O. (2004). In vivo investigation of the transcription, processing, endonucleolytic activity, and functional relevance of the spatial distribution of a plant miRNA. Genes Dev. *18*, 2237–2242.

Peragine, A., Yoshikawa, M., Wu, G., Albrecht, H.L., and Poethig, R.S. (2004). *SGS3* and *SGS2/SDE1/RDR6* are required for juvenile development and the production of *trans*-acting siRNAs in *Arabidopsis*. Genes Dev. *18*, 2368–2379.

Rhoades, M.W., Reinhart, B.J., Lim, L.P., Burge, C.B., Bartel, B., and Bartel, D.P. (2002). Prediction of plant microRNA targets. Cell *110*, 513–520.

Ronemus, M., Vaughn, M.W., and Martienssen, R. (2006). MicroRNA-targeted and small interfering RNA–mediated mRNA degradation is regulated by Argonaute, Dicer, and RNA-dependent RNA polymerase in *Arabidopsis*. Plant Cell *18*, 1559–1574.

Schwab, R., Palatnik, J.F., Riester, M., Schommer, C., Schmid, M., and Weigel, D. (2005). Specific effects of microRNAs on the plant transcriptome. Dev. Cell *8*, 517–527.

Smith, H.A., Swaney, S.L., Parks, T.D., Wernsman, E.A., and Dougherty, W.G. (1994). Transgenic plant virus resistance mediated by untranslatable sense RNAs: Expression, regulation, and fate of nonessential RNAs. Plant Cell *6*, 1441–1453.

Sunkar, R., and Zhu, J.K. (2004). Novel and stress-regulated microRNAs and other small RNAs from *Arabidopsis*. Plant Cell *16*, 2001–2019.

Tang, G., Reinhart, B.J., Bartel, D.P., and Zamore, P.D. (2003). A biochemical framework for RNA silencing in plants. Genes Dev. *17*, 49–63.

Vazquez, F., Gasciolli, V., Crete, P., and Vaucheret, H. (2004a). The nuclear dsRNA binding protein HYL1 is required for microRNA accumulation and plant development, but not posttranscriptional transgene silencing. Curr. Biol. *14*, 346–351.

Vazquez, F., Vaucheret, H., Rajagopalan, R., Lepers, C., Gasciolli, V., Mallory, A.C., Hilbert, J.L., Bartel, D.P., and Crete, P. (2004b). Endogenous *trans*-acting siRNAs regulate the accumulation of *Arabidopsis* mRNAs. Mol. Cell *16*, 69–79.

Williams, L., Carles, C.C., Osmont, K.S., and Fletcher, J.C. (2005). A database analysis method identifies an endogenous trans-acting short-interfering RNA that targets the *Arabidopsis ARF2, ARF3*, and *ARF4* genes. Proc. Natl. Acad. Sci. USA *102*, 9703–9708.

Xie, Z., Allen, E., Wilken, A., and Carrington, J.C. (2005). DICER-LIKE 4 functions in trans-acting small interfering RNA biogenesis and vegetative phase change in *Arabidopsis thaliana*. Proc. Natl. Acad. Sci. USA *102*, 12984–12989.

Yoshikawa, M., Peragine, A., Park, M.Y., and Poethig, R.S. (2005). A pathway for the biogenesis of *trans*-acting siRNAs in *Arabidopsis*. Genes Dev. *19*, 2164–2175.

Zamore, P.D., and Haley, B. (2005). Ribo-gnome: the big world of small RNAs. Science *309*, 1519–1524.

Accession Numbers

The consensus sequences of *PpTAS1-4* were deposited in Genbank (BK005825, BK005826, BK005827, and BK005828). 127,135 unique, genome-matched *P. patens* and 340,114 unique, genome-matched *Arabidopsis* small RNAs were deposited with the Gene Expression Omnibus (GSE5103 and GSE5228, respectively). The sequences of the *P. patens* and *Arabidopsis* small RNAs analyzed in this study are also available in Supplemental Databases S1 and S2, respectively.